

ESTIMATION OF NOISE RADIATED DUE TO THE FLOW IN MACHINES USING COMPUTATIONAL FLUID DYNAMICS

Bhanuprakash TALLAPRAGADA¹ and Ramesh KOLLURU²

¹ Dept of Marine Engineering, College of Engineering, Andhra University, Visakhapatnam, India

² Dept of Mechanical Engineering, Al-Ameer College of Engineering, Visakhapatnam, India

ABSTRACT

Heavy-duty motors are used in marine applications for supplying cooling water to internal combustion engines, seawater to ballast tanks, and for sewage operations. Cooling of these heavy-duty electric motors is an important issue concerning the performance of the motor. Heat is dissipated from the motor surface via conduction, convection and radiation. For enhancing heat transfer rate, fins are provided thereby increasing the effective area of cooling. Owing to the space constraints in marine applications a cooling fan is mounted integral to the motor shaft to facilitate the motor with forced convection cooling. In this work, suitability of mixed flow fan for heavy-duty motors is studied using CFD for flow optimization. The results of CFD are used for prediction of the radiated noise. The CFD code prediction of noise levels is found to meet design criteria of 70dB.

INTRODUCTION

Heavy-duty motors find applications in submarines and ships for transporting fluids for various applications. During the design of these motors, a very important factor that needs to be considered is the high temperatures encountered during the operation. Cooling of these heavy-duty motors is done by providing a fan-mounted integral to the motor shaft or by means of an external fan. The cooling fan must supply adequate air that is drawn from circular inlet into cowl containing the fan. This air must then be forced along the ribs mounted on the motor and traverse the length of the motor for effective heat transfer. Owing to the space constraints in marine applications, preference is given to the fan-mounted integral to the motor shaft. Limitations imposed by standards on the geometry of the motor lead to a severe restriction on the geometry of the fan and thus on the flow path of the cooling air.

The basic parameters in designing a fan are the flow rate and Pressure Head. Apart from the basic parameters, speed of the fan, type of fan, and size of the fan must match to ensure higher efficiency and better performance. Owing to the combinations of these three variables namely Pressure Head, Discharge Head and size of the fan, a convergent solution is not possible unless one or two of them are fixed during the design process. Important factors, which are to be checked in design of a fan are, adequate flow rate, the direction of the flow and the noise generated by the fan which has a drastic effect on the ambience especially in marine applications.

SELECTION OF TYPE OF FAN

Selection of a fan mainly relies on "specific speed" curves, to indicate first the type of fan. Centrifugal fans are used where high pressure is the main criterion whereas an axial flow fan is used where high volume flow is required. Mixed flow fan

lies in-between the centrifugal fan and axial flow fan satisfying both the pressure and volume flow requirements.

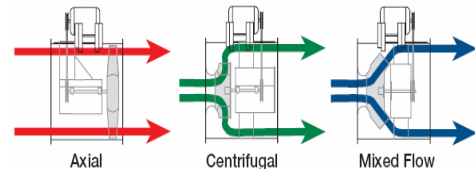


Figure 1: Flow directions for different types of fan [1]

Fig. 1 shows the air flow paths for the three types of fans considered. For an axial flow fan the direction of air flow from inlet to outlet is axial. For a centrifugal fan air flow is axial at the inlet and it is turned up by ninety degrees at the outlet. For a mixed flow fan the direction of airflow at exit is at an angle determined by the fan geometry. For diverting the flow over the ribs of the motor, a centrifugal fan must be provided with an external cap. This cap gets excited during the operation of the fan and adds to the total radiated noise. An axial flow fan does not require an external cap whereas for a mixed flow fan, the cap acts mostly as a safety device.

Fig. 2 compares the noise levels characteristics of the three fans without an external cap [1]. The most disturbing frequency for human ear lies between 1000 Hz and 3000 Hz. In this range the centrifugal fan produces the least noise, axial flow fan the highest and the mixed flow fan lies between these two extremes. But the external cap necessary for diverting the flow over the ribs in the case of a centrifugal fan offsets the low noise levels and is not suitable for the present application. Thus a mixed flow fan is selected whose noise radiation characteristics lie in between the two extremes but in which the external cap does not have an appreciable noise augmentation.

SOURCES OF NOISE

The sources of noise in a fan are the following [2].

- The pressure field over the surface of the blades in rotating space.
- Turbulent boundary layer pressure perturbations, at high Reynolds numbers. These perturbations radiate broadband noise whose intensity depends on the amplitude of the pressure oscillations and the ratio of their correlated wavelength to the dimensions of the radiating surface of the blade.
- The flow over the fan blades causes cyclic excitation by the presence of obstacles such as inlet cowls, mounting lugs, and ribs. Depending on the rotational speed of the fan and the number of blades and obstacles, this situation can give rise to tones.
- The other sources include
 - Vortices generated over the tips of the blades close to the cowl and in the plenum chamber,

- Separated flow over the ribs particularly near to the efflux from the cowl,
- Flow noise from the air passing over the grid in the inlet of the cowl.

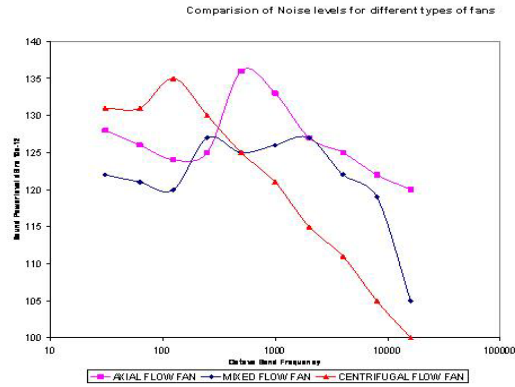


Figure 2: Noise levels of various fans [1]

NUMERICAL TECHNIQUE

In the present work the suitability of a mixed flow fan for heavy-duty motors, mounted integral with the motor shaft is studied using CFD for flow optimization. Analysis is also carried out to estimate the noise levels radiated by mixed flow fan using Fluent, a commercially available CFD code.

The governing equations of mass conservation and momentum conservation are described by

$$\frac{\partial \rho}{\partial t} + \nabla \cdot (\rho \mathbf{v}) = S_m$$

$$\frac{\partial (\rho \mathbf{v})}{\partial t} + \nabla \cdot (\rho \mathbf{v} \mathbf{v}) = -\nabla p + \nabla \cdot (\boldsymbol{\tau}) + \rho \mathbf{g}$$

Where p is the static pressure, $\boldsymbol{\tau}$ is the stress tensor (described below), and $\rho \mathbf{g}$ and \mathbf{F} are the gravitational body force and external body forces.

$$\boldsymbol{\tau} = \mu \left[\nabla \mathbf{v} + \nabla \mathbf{v}^T - \frac{2}{3} \nabla \cdot \mathbf{v} \mathbf{I} \right] \text{ where } \mu \text{ is the molecular}$$

viscosity, \mathbf{I} is the unit tensor, and the second term on the right hand side is the effect of volume dilation. The turbulence kinetic energy, k , and its rate of dissipation, ε , are obtained from the following transport equations:

$$\frac{\partial (\rho k)}{\partial t} + \frac{\partial (\rho k u_i)}{\partial x_i} = \frac{\partial}{\partial x_j} \left[\left(\mu + \frac{\mu_t}{\sigma_k} \right) \frac{\partial k}{\partial x_j} \right] + G_k + G_b - \rho \varepsilon - Y_M + S_k$$

and

$$\frac{\partial (\rho \varepsilon)}{\partial t} + \frac{\partial (\rho \varepsilon u_i)}{\partial x_i} = \frac{\partial}{\partial x_j} \left[\left(\mu + \frac{\mu_t}{\sigma_\varepsilon} \right) \frac{\partial \varepsilon}{\partial x_j} \right] + C_{1\varepsilon} \frac{\varepsilon}{k} (G_k + C_{3\varepsilon} G_b) - C_{2\varepsilon} \rho \frac{\varepsilon^2}{k} + S_\varepsilon$$

In these equations, G_k represents the generation of turbulence kinetic energy due to the mean velocity gradients, G_b is the generation of turbulence kinetic energy due to buoyancy, Y_M represents the contribution of the fluctuating dilatation in compressible turbulence to the overall dissipation rate. $C_{1\varepsilon}$, $C_{2\varepsilon}$, and $C_{3\varepsilon}$ are constants. σ_k and

σ_ε are the turbulent Prandtl numbers for k and, ε respectively. S_k and S_ε are user-defined source terms. A 3-D unsteady case with Large Eddy simulation as viscous model and Smagorinsky-Lilly model as sub grid model is used to solve the governing equations. A standard pressure model is used for discretization of pressure. The SIMPLE algorithm is used for pressure-velocity coupling and the momentum is discretized by second-order momentum scheme.

The results of the CFD analysis are taken as input for the acoustic predictions. The model used for noise radiated due to the flow of air is the Ffowcs Williams Model. The Ffowcs Williams and Hawkings (FW-H) equation is essentially an inhomogeneous wave equation that is derived by manipulating the continuity equation and the Navier-Stokes equations and is given by

$$\frac{1}{a_o^2} \frac{\partial^2 \mathbf{p}'}{\partial t^2} - \nabla^2 \mathbf{p}' = \frac{\partial^2}{\partial x_i \partial x_j} \{ T_{ij} H(\mathbf{f}) \}$$

$$- \frac{\partial}{\partial x_i} \{ [P_{ij} n_j + u_i \rho (\mathbf{u}_n - \mathbf{v}_n)] \delta(\mathbf{f}) \}$$

$$+ \frac{\partial}{\partial t} \{ [\rho_o \mathbf{v}_n + \rho (\mathbf{u}_n - \mathbf{v}_n)] \delta(\mathbf{f}) \} \rightarrow 1$$

u_i = Fluid velocity component in the x_i direction

u_n = Fluid velocity component normal to the surface

v_i = Surface velocity components in x_i direction

v_n = Surface velocity component normal to the surface

$\delta(f)$ = Dirac delta function

$H(f)$ = Heaviside function

$T_{ij} = \rho u_i u_j + P_{ij} - a_o^2 (\rho - \rho_o) \delta_{ij}$ is the Lighthill tensor.

P_{ij} is compressive stress tensor, for stokesian fluid this is given by

$$p \delta_{ij} - \mu \left[\frac{\partial u_i}{\partial u_j} + \frac{\partial u_j}{\partial u_i} - \frac{2}{3} \frac{\partial u_k}{\partial x_k} \delta_{ij} \right]$$

This model considers time-accurate solutions of the flow-field variables, such as pressure, velocity components, and density on source (emission) surfaces to evaluate the surface integrals. These parameters are obtained from large eddy simulation (LES) flow model, which determines the flow field.

MODEL CREATION AND GRID GENERATION

Fig. 3 shows the side view of the solid model of fan integral with motor. Commercially available software ICEMCFD is used for generating the grid. The outer domain considered is 5 times the fan diameter. This is shown in Fig. 4. Owing to the complexity of the geometry, a tetrahedral grid was used for the CFD analysis. The total number of tetrahedral cells was of the order of half million cells.

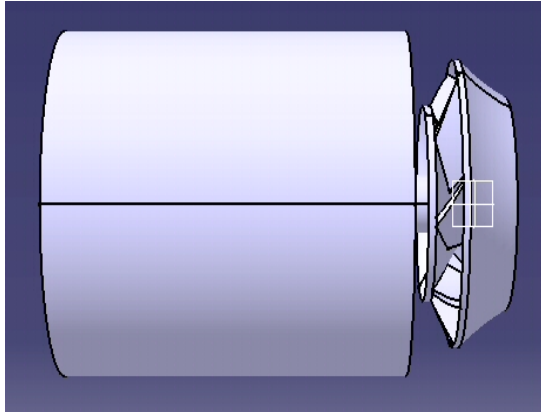


Figure 3: Side view of the fan integral with motor

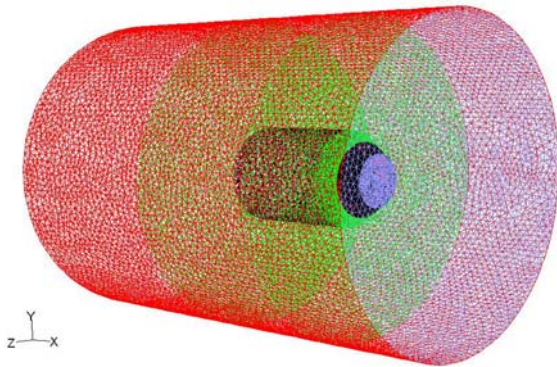


Figure 4: Tetrahedral Grid of the entire domain

RESULTS AND DISCUSSION

Figure 6 shows the flow velocity contours over the fan. The tangential velocity of the air at the outlet is 35.5 m/s that agrees well with the theoretical value of 35.5 m/s exactly. Zhou et. Al [3] predicted a reverse flow to occur near the inlet, which was substantiated by their experiments. Fig. 7 shows the static pressure contours on the fan. This distribution of the pressure on the fan is used in estimation of noise for the fan. Figure 9 shows show the velocity vectors of the flow field. It can be seen that outlet velocity vector is at an angle to the inlet velocity vector indicating that the flow can be easily diverted on to the motor when compared to the flow from a centrifugal fan. A reverse flow can be seen at the inlet as shown by the direction of the velocity vectors. This validates the theoretical prediction using numerical technique and also verified by experiments [4].

Table 1 shows the flow rate in kg/s from the mixed flow fan with different number of blades. The seven bladed fan produces a mass flow rate of 0.5 kg/s which is the design value. Figure 9 shows the path lines emerging from the fan on to the motor surface with out the safety cap on the fan. This validates the flow optimization.

PREDICTIONS OF NOISE RADIATION:

The noise radiated from the fan at different receiver locations in (x,y,z) directions are calculated and are plotted. Fig. 10 a-d shows the Fast Fourier Transform of sound pressure level plotted is against the frequency. The plots show the noise

levels for a seven bladed fan at various receiver locations. Fig 10 a shows the noise radiated from the fan at receive location of (1 5 5) m from the fan and the over all sound pressure level at this distance is 66.17 dB. Fig 10 b shows the noise radiated from the fan at receive location of (1 4 4) m from the fan and the over all sound pressure level at this distance is 77.71 dB. Fig 10 c shows the noise radiated from the fan at receive location of (1 3 3) m from the fan and the over all sound pressure level at this distance is 78.80 dB. Fig 10 d shows the noise radiated from the fan at receive location of (1 2 2) m from the fan and the over all sound pressure level at this distance is 88.07 dB. The noise levels are close to the standard values from literature [1,2]. The noise radiated from six and eight bladed fans showed similar results and are not presented here.

| Mass Flow Rate (kg/s) | Six | Seven | Eight |
|-----------------------|------|-------|-------|
| Shroud outflow | 0.58 | 0.5 | 0.438 |

Table 1: Mass Flow rate from CFD ANALYSIS

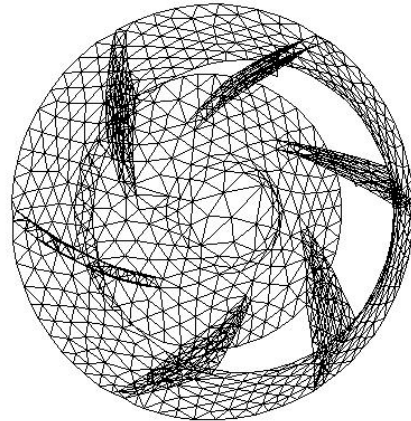


Figure 5a: Computational grid for six bladed Fans

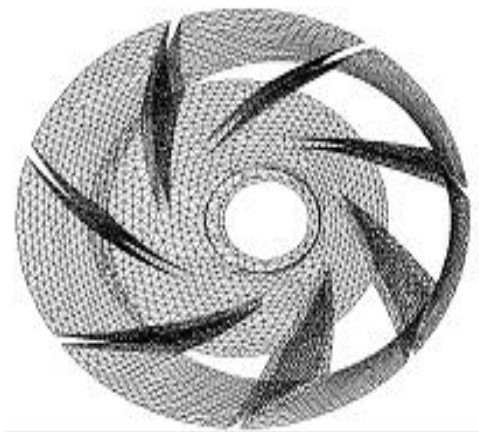


Figure 5b: Computational domain for seven bladed Fan.

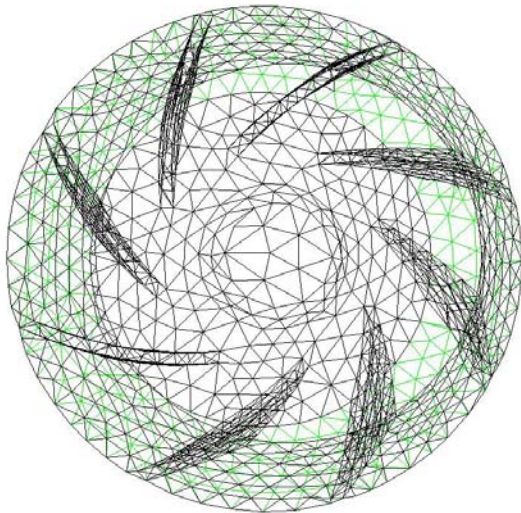


Figure 5c: Computational domain for eight bladed Fan.

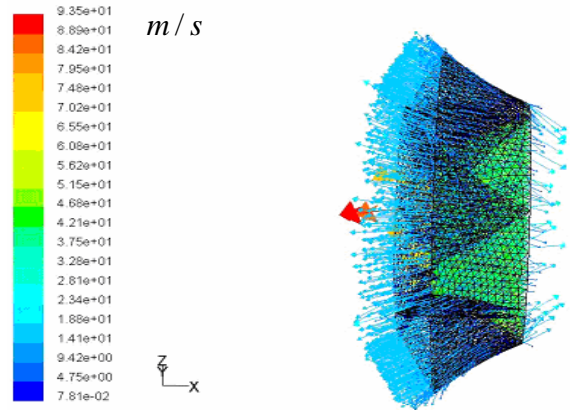


Figure 8: Velocity vectors for the fan.

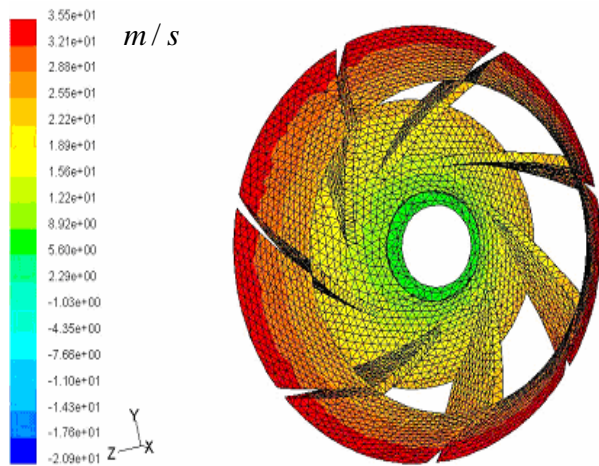


Figure 6: Velocity Contours of the fan

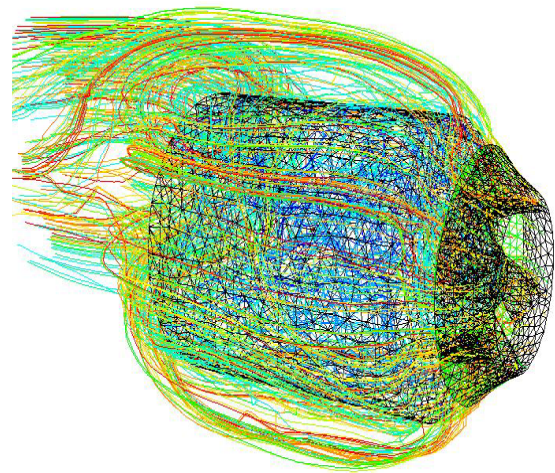


Figure 9: Paths lines from the fan on to the motor

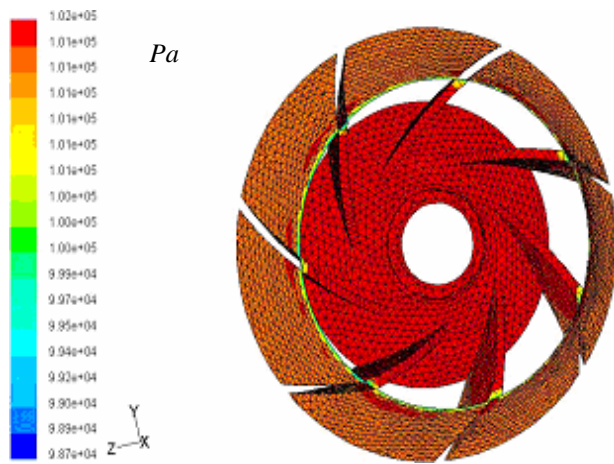
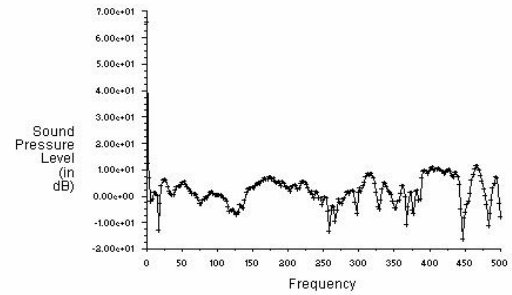
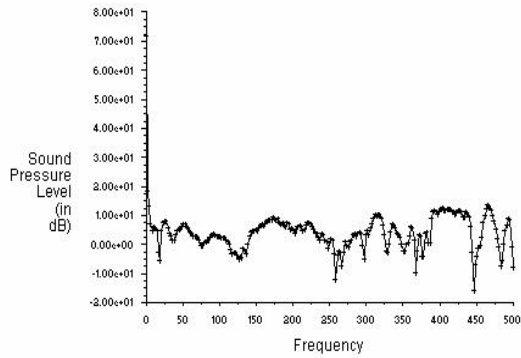


Figure 7: Static Pressure distribution on the fan



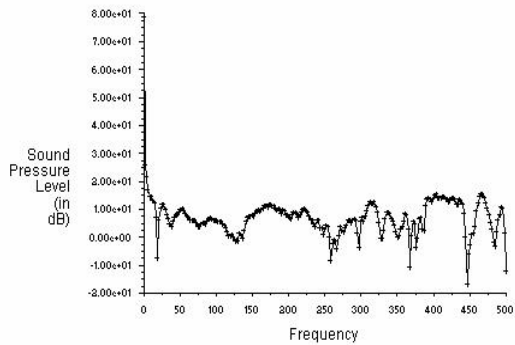
Spectral Analysis of Pressure at receiver-5 (Time=5.2000e-01) FLOW1 6.1 (3d, dp, segregated, LES, unsteady) Apr 25, 2006

Figure 10a: SPL Vs frequency at receiver position of (1,5,5) m for 7 bladed fan



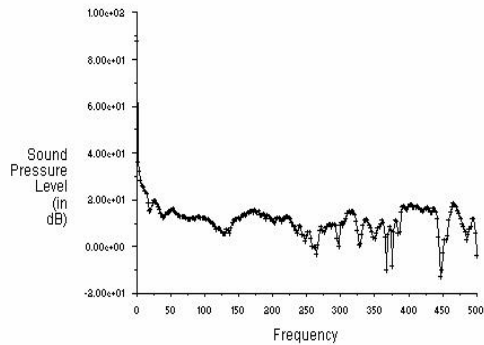
Spectral Analysis of Pressure at receiver-4 (Time=5.2000e-01) Apr 25, 2006
 FLUENT 6.1 (3d, dp, segregated, LES, unsteady)

Figure 10b: SPL Vs frequency at receiver position of (1, 4, 4) m for 7 bladed fan



Spectral Analysis of Pressure at receiver-3 (Time=5.2000e-01) Apr 25, 2006
 FLUENT 6.1 (3d, dp, segregated, LES, unsteady)

Figure 10c: SPL Vs frequency at receiver position of (1,5,5) m for 7 bladed fan



Spectral Analysis of Pressure at receiver-2 (Time=5.2000e-01) Apr 25, 2006
 FLUENT 6.1 (3d, dp, segregated, LES, unsteady)

Figure 10d: SPL Vs Frequency at receiver position of (1,2,2) m for seven bladed fan.

CONCLUSION

A heavy-duty motor for marine applications is considered. A cooling fan integral with the motor is analysed using CFD. The fan is designed such that the cooling air drawn into a cowl is discharged over ribs distributed on the casing with

out much impact on the cover enclosing the fan there by allowing the reduction of noise resulting from vibration of the cover. The flow paths of air for a mixed flow fan with 6, 7 and 8 blades are obtained using Fluent. The flow path lines obtained are found to be optimum. The six bladed fans have a higher mass flow rate compared to the other two configurations. The CFD analysis is then extended to estimate noise at different positions for the three models considered. The sound pressure levels for all the three cases are below the maximum accepted levels of 85-90 dB at all frequencies of interest. A slight increase in noise levels is observed for higher number of blades with a corresponding decrease in mass flow rates which can be related to increase in blade past frequency.

REFERENCES

1. How the mixed flow fan works, document by Green Heck Company.
2. Mathur, J. S. B, Basic requirements of low noise cooling fans.
3. Weidong Zhou, Zhimei Zhao, T. S. Lee, and S. H. Winoto, (2003) Investigation of Flow Through Centrifugal Pump Impellers Using Computational Fluid Dynamics, *International Journal of Rotating Machinery*, 9(1): 49–61.